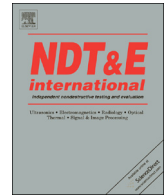




ELSEVIER

Contents lists available at ScienceDirect

NDT&amp;E International

journal homepage: [www.elsevier.com/locate/ndteint](http://www.elsevier.com/locate/ndteint)

# Numerical simulation and experiment for inspection of corner-shaped components using ultrasonic phased array

Na Xu <sup>a,\*</sup>, Zhenggan Zhou <sup>b</sup><sup>a</sup> Beijing Institute of Aeronautical Materials, Aviation Industry Corporation of China, Beijing 100095, China<sup>b</sup> School of Mechanical Engineering and Automation, Beihang University, Beijing 100191, China

## ARTICLE INFO

### Article history:

Received 27 December 2012

Received in revised form

31 December 2013

Accepted 21 January 2014

Available online 29 January 2014

### Keywords:

Phased array

Ultrasonic testing

Corner-shaped

Finite-difference time domain

Simulation

## ABSTRACT

This paper proposes an effective method for corner-shaped components inspection using ultrasonic phased array. We first improved the finite-difference time domain (FDTD) method by way of averaging properly the different ultrasonic parameters of media on the both sides of interface to simulate ultrasonic wave propagation in dual-layered media. Then, an inspection method for corner-shaped structures using ultrasonic phased array and an iterative calculation approach of delay time based on Snell's law for complicated geometries were put forward and described in detail. Experiments on an aluminum alloy 2014 sample were conducted to validate the modeling results and the inspection method. Finally, practical application was carried out to image and size the defect in carbon fiber reinforced plastic (CFRP) corner-shaped specimen, yielding experiment results that are in good quantitative agreement with the true values.

© 2014 Elsevier Ltd. All rights reserved.

## 1. Introduction

Corner-shaped components, such as spars, strings and top-hat structures, have been widely applied in aerospace industry in recent years. Since the equivalent stress is mainly concentrated in and around the radius parts, the reliability of these structures could be seriously compromised by flaws introduced during manufacture, such as delamination, debonding and fiber breakage [1]. It is thus imperative to develop a rapid and effective flaw inspection method for corner-shaped components used in aerospace industry. However, the ultrasonic inspection method using conventional monolithic transducers, when used on such components, could lead to degradation of performance mainly due to several inherent disadvantages including uncovered scanning area, wave beam disorientations and distortions. By contrast, ultrasonic phased array technique, which provides improved sensitivity and advantageous flexibility, can be used to overcome these difficulties in nondestructive testing (NDT) industry [2].

Ultrasonic array transducer is composed of multiple piezoelectric elements excited with properly time-delayed pulses to sweep the wave beams over the interesting area of the specimen, such that the wavefronts of all the individually delayed signals will then form Huygens' interference patterns. By phasing each array element its relative transmission time, the parameters of wave

beams such as focus depths and steering angles could be adjusted, leading to improved capability of imaging defects located in regions difficult to access. Furthermore, the near real-time electronic scanning can be used to replace the manual or automated motion of conventional monolithic transducer for better efficiency, and the shape of the array transducer can be customized to match the specimen geometry. Previous studies of ultrasonic phased array technique applied in NDT include inspection of titanium forgings in aerospace industry [3], low-pressure turbine discs [4] and welds [5] in nuclear power plant.

Considering the costly and intricate set-up as well as the time-consuming experimental procedure, it is unfeasible to conduct NDT experiments by applying the ultrasonic phased array method on a large number of test specimens with various geometrical shapes. On the other hand, the FDTD method, as one of the most powerful and versatile numerical analysis techniques, has been proved to be especially suitable to simulate propagation of ultrasonic wave in a test specimen and its interaction with internal defects [6]. In this study, the FDTD method was used to simulate the whole process of ultrasonic waves generation and reception so as to optimize inspection parameters such as focus depths and steering angles.

This paper is arranged in the following manner. We firstly improve the stability of the traditional FDTD formulation by averaging material ultrasonic parameters on both sides of the material interface. Then the scheme of the corner-shaped component inspection method is presented and the calculation of delay time is elaborated. Subsequently, a 2-dimensional implementation

\* Corresponding author. Tel./fax: +86 10 8231 3466.  
E-mail address: [bjxuna@163.com](mailto:bjxuna@163.com) (N. Xu).

of the improved FDTD method is performed to image and locate the internal defect in a 30 mm thick aluminum alloy 2014 corner-shaped test specimen. Finally, the experiment for a CFRP corner-shaped specimen with an artificial delamination defect (10 mm × 5 mm film) is conducted using a 5 MHz, 32 elements linear array transducer to verify the correctness of the inspection method.

## 2. Improved FDTD formulation

One of the key issues with numerical algorithms that must be considered is numerical stability [7]. The fundamental condition for the stability of finite-difference algorithm, which relates the size of the time increment to the spacing of the discrete nodes in the FDTD grid is the well-known Courant stability condition. In traditional FDTD algorithm, the finite-difference algorithm is stable in most cases when the Courant condition is satisfied. For corner-shaped component, the inspection surfaces of specimen are irregular so that the linear array probes cannot be simply applied in direct contact. To solve this problem, typically a water path or specially profiled wedge has to be used to couple the array. In this case, ultrasonic waves emitted from probe have to propagate through two distinct media: the coupling layer and specimen. However, when there are remarkable differences between the ultrasonic properties (such as wave speed and density) of the two adjacent media, the traditional FDTD algorithm turns out to be unstable based on the Courant stability condition, and a more restrictive condition for the stability need to be imposed [8].

In this section, we show that the conventional FDTD algorithm can be improved by way of averaging properly the ultrasonic parameters of media on the both sides of interface, so that the Courant condition sufficient condition for stability and no other conditions will be needed.

### 2.1. Wave equation

The 2-dimensional FDTD algorithm for the simulation of elastic wave propagation is based on a first order velocity–stress finite-difference method. The elastic wave equations [9] are given by

$$\rho \frac{\partial v_x}{\partial t} = \frac{\partial \sigma_{xx}}{\partial x} + \frac{\partial \sigma_{xz}}{\partial z} \quad (1)$$

$$\rho \frac{\partial v_z}{\partial t} = \frac{\partial \sigma_{xz}}{\partial x} + \frac{\partial \sigma_{zz}}{\partial z} \quad (2)$$

$$\frac{\partial \sigma_{xx}}{\partial t} = C_{11} \frac{\partial v_x}{\partial x} + C_{13} \frac{\partial v_z}{\partial z} \quad (3)$$

$$\frac{\partial \sigma_{zz}}{\partial t} = C_{13} \frac{\partial v_x}{\partial x} + C_{33} \frac{\partial v_z}{\partial z} \quad (4)$$

$$\frac{\partial \sigma_{xz}}{\partial t} = C_{55} \left( \frac{\partial v_x}{\partial z} + \frac{\partial v_z}{\partial x} \right) \quad (5)$$

Here,  $v_x$  and  $v_z$  are the velocity vectors;  $\sigma_{xx}$ ,  $\sigma_{zz}$  and  $\sigma_{xz}$  are the stress tensors;  $\rho$  is the medium density;  $C_{11}$ ,  $C_{13}$ ,  $C_{33}$  and  $C_{55}$  are the medium elastic constants. For a homogeneous isotropic material, the elastic constants can be expressed as

$$\begin{cases} C_{11} = C_{33} = \lambda' + 2\mu' \\ C_{13} = \lambda' \\ C_{55} = \mu' \end{cases} \quad (6)$$

Here,  $\lambda'$  and  $\mu'$  are Lamé's constants.

The finite-difference discretization of the set of equations leads to a staggered finite-difference grid [10], as shown in Fig. 1. Here, the space is discretized into a set of points uniformly spaced in each direction with integer or semi-integer multiples of distance intervals  $\Delta x$  and  $\Delta y$ , and similarly the time into instants with

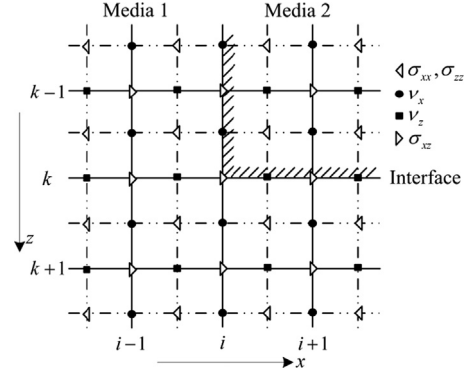


Fig. 1. 2-Dimensional finite-difference grid.

integer and semi-integer multiples of a given time interval  $\Delta t$ .  $\sigma_{xx}$  and  $\sigma_{zz}$  represent normal stresses at the nodes, whereas the velocity variables  $v_x$  and  $v_z$ , as well as the shear component  $\sigma_{xz}$  are variables on the grid half-spatial steps away from the nearest node. The velocity and stress components in the grid are unknowns offset by  $\Delta t/2$  in time domain. This leads to a leap-frog scheme in which the velocity components are calculated during the first half-time step  $\Delta t/2$ , then stress components are updated in the next half-time step. In the next  $\Delta t/2$ , the velocity components at  $\Delta t + \Delta t/2$  are calculated using the stress components updated at the end of the first time step  $\Delta t$ .

### 2.2. Improving the FDTD formulation

In order to enhance the stability of the finite-difference algorithm for elements on the interface of two remarkably different materials, the two material parameters are averaged for the field components on both sides of the interface. A part of 2-dimensional finite-difference grid across two different media is shown in Fig. 1. The velocity component  $v_x$  lies on the vertical boundary, whereas  $v_z$  is placed on the horizontal boundary. The only stress component that is placed on the boundary is the shear stress  $\sigma_{xz}$ . A linear averaging procedure is presented which is derived in a straightforward manner from the governing equations in integral form.

The velocity components are firstly considered for the horizontal particle velocity  $v_x$ , the procedure for averaging the material density on vertical boundary is derived from Eq. (1).

$$\iint_{\text{Box}} \rho \frac{\partial v_x}{\partial t} dx dz = \iint_{\text{Box}} \left[ \frac{\partial \sigma_{xx}}{\partial x} + \frac{\partial \sigma_{xz}}{\partial z} \right] dx dz \quad (7)$$

where the integration is carried out over a rectangular area equivalent to the size of one box of the finite-difference grid. The horizontal and vertical ranges of integration are

$$\begin{cases} (i-1/2)dx \leq x \leq (i+1/2)dx \\ (k-1)dz \leq z \leq kdz \end{cases}$$

where  $i, k = 1, 2, \dots, N$  are the node indices of the 2D grid.

This integral is then discretized into the following difference function.

$$\rho_{\text{avg}} \frac{v_x|_{i,k-1/2}^{n+1/2} - v_x|_{i,k-1/2}^{n-1/2}}{T} = \frac{\sigma_{xx}|_{i+1/2,k-1/2}^n - \sigma_{xx}|_{i-1/2,k-1/2}^n}{\Delta x} + \frac{\sigma_{xz}|_{i,k}^n - \sigma_{xz}|_{i,k-1}^n}{\Delta z} \quad (8)$$

$$\rho_{\text{avg}} = \frac{\rho_{i-1/2,k-1/2} + \rho_{i+1/2,k-1/2}}{2} \quad (9)$$

The material densities of the two media are thus linearly averaged for the velocity components on the boundary and the vertical velocity  $v_z$  is arranged in the same way.

Download English Version:

<https://daneshyari.com/en/article/295085>

Download Persian Version:

<https://daneshyari.com/article/295085>

[Daneshyari.com](https://daneshyari.com)